

BURSTING ACTIVITY IN NEOCORTICAL NETWORKS

THE ROLE OF PERSISTENT SODIUM CURRENT IN BURSTING
ACTIVITY OF MOUSE NEOCORTICAL NETWORKS IN VITRO

Running Head:

BURSTING ACTIVITY IN NEOCORTICAL NETWORKS

Wim van Drongelen,^{1,2} Henner Koch,³ Frank P. Elsen,¹ Hyong C. Lee,¹Ana Mrejeru,³ Erin Doren,¹ Charles J. Marcuccilli,¹ Mark Hereld,^{2,4}Rick L. Stevens,^{2,4} and Jan-Marino Ramirez³¹Department of Pediatrics, The University of Chicago, Chicago, IL²Computation Institute, The University of Chicago, Chicago, IL³Department of Anatomy and Organismal Biology, The University of Chicago, Chicago, IL⁴Mathematics and Computer Science Division, Argonne National Laboratory, Argonne, ILContact Information:

Wim van Drongelen

Department of Pediatrics, C372, MC 3055,
5841 S. Maryland Avenue, Chicago, IL. 60637-1470.

Tel: (773) 834 9049

Fax: (773) 702 4786

E-mail: wvandron@peds.bsd.uchicago.edu

BURSTING ACTIVITY IN NEOCORTICAL NETWORKS

ABSTRACT

Most types of electrographic epileptiform activity can be characterized by isolated or repetitive bursts in brain electrical activity. This observation is our motivation to determine mechanisms that underlie bursting behavior of neuronal networks. Here we show that the persistent sodium current (I_{NaP}) in mouse neocortical slices is associated with cellular bursting, and our data suggests that these cells are capable of driving networks into a bursting state. This conclusion is supported by the following observations:

1. Voltage clamp measurements show that riluzole (20 μ M) and very low concentrations of TTX (50 nM) attenuate I_{NaP} currents in the neural membrane within a one-minute interval after bath application of the drug.
2. Recordings of synaptic activity demonstrate that riluzole at this concentration does not affect postsynaptic properties.
3. Both low concentrations of TTX and riluzole reduce and eventually stop network bursting while they simultaneously abolish intrinsic bursting properties and sensitivity levels to electrical stimulation in individual intrinsically bursting cells.
4. The sensitivity levels of regular spiking neurons are not significantly affected by riluzole or TTX at the termination of network bursting.
5. Propagation of cellular bursting in a neuronal network depended on excitatory connectivity and disappeared upon bath application of CNQX [20 μ M] + CPP [10 μ M].
6. Simulations with a neocortical network model including different types of pyramidal cells, inhibitory interneurons, neurons with and without I_{NaP} currents, and recurrent excitation, confirm the essence of our experimental observations that I_{NaP} conductance can be a critical factor sustaining slow population bursting.

Keywords: Epilepsy, Bursting, Computational Modeling

BURSTING ACTIVITY IN NEOCORTICAL NETWORKS

INTRODUCTION

Epilepsy is a common neurological disease characterized by chronic seizures, affecting ~1% of the world population. Seizure activity in the neocortex plays a major role in children with intractable epilepsy, and a better understanding of neocortical physiology is critical for the development of a rational approach to anticonvulsant therapy. One of the major characteristics of most types of epileptiform behavior is a rhythmic pattern of electrical discharges of the neuronal population. In principle these discharges may be caused by intrinsic neuronal mechanisms, network function, or—most likely—both network and cellular properties. Increasing evidence suggests that epileptiform activity originates within the neocortex (Timofeev and Steriade 2004). When considering network bursting and different cell types known to occur in neocortex, the intrinsically bursting cell type (Connors and Gutnick 1990; Gray and McCormick 1996; Steriade et al. 1998) seems especially interesting. Intrinsically bursting neurons, in particular the so-called fast rapid bursting neurons have been hypothesized to play an important role in epileptogenesis and various forms of neocortical activity (Blatow et al. 2003; Cunningham et al. 2004; Timofeev and Steriade 2004). In animal models it was established that intrinsically bursting neurons are increased in seizing tissue (Jacobs et al. 1999; Sanabria et al. 2002; Steriade et al. 2001; Timofeev et al. 2000). Indeed, recent evidence indicates that this cell type occurs in neocortex of pediatric patients with epilepsy (Foehring and Wyler 1990; Van Drongelen et al. 2003b). The simplest scenario is a unidirectional path from cell to network, where a bursting neuron paces the activity of a neuronal population. This “pacemaker hypothesis” was first raised in 1949, when Bremer postulated that neurons with intrinsic pacemaker or bursting properties contribute

BURSTING ACTIVITY IN NEOCORTICAL NETWORKS

1
2
3 to the generation of neocortical EEG activity (Bremer 1949). However, a better
4
5 understanding of how neuronal networks generate rhythmic activity led to a major
6
7 modification of a pure “pacemaker hypothesis” as several studies indicated that bursting
8
9 and synaptic properties interact in concert. Unfortunately, the close interaction between
10
11 these properties makes it extremely difficult or even impossible to determine the relative
12
13 contribution of these properties in functional neuronal networks. The finding that the
14
15 strength of synaptic and intrinsic bursting properties is not fixed but dynamically
16
17 modulated by endogenously released neuromodulators or by manipulations such as
18
19 deafferentiation further complicates the question to what extent intrinsic and synaptic
20
21 properties contribute to rhythm generation (Foehring et al. 2002; Peña and Ramirez 2004;
22
23 Topolnik et al. 2003).

24
25
26
27
28
29 The difficulty of determining the relative contribution of synaptic and bursting
30
31 properties to the generation of a given activity pattern was overcome in some small
32
33 invertebrate neuronal networks, which were particularly amenable to a rigorous cellular
34
35 and systems level analysis (Marder and Calabrese 1996). The increased difficulty of
36
37 dissecting synaptic and bursting properties in mammalian networks created considerable
38
39 uncertainty as to how intrinsic and synaptic properties interact to generate rhythmic
40
41 activity. This is an issue of general interest because bursting neurons exist almost
42
43 everywhere in the mammalian nervous system (Ramirez et al. 2004) including the
44
45 thalamus, basal ganglia, spinal cord (Darbon et al. 2004), medulla (Peña and Ramirez
46
47 2004), hypothalamus, olfactory bulb, ventral tegmentum, hippocampus (Sanabria et al.
48
49 2001), and neocortex (Connors and Gutnick 1990; Dégenétais et al. 2003; Istvan and
50
51 Zarzecki 1994; Nowak et al. 2003). While some researchers hypothesize that these
52
53
54
55
56
57
58
59
60

BURSTING ACTIVITY IN NEOCORTICAL NETWORKS

1
2
3 neurons are primarily responsible for the generation of rhythmic activity in areas where
4
5
6 bursting neurons are found (for a review see Arshavsky 2003), other studies suggest that
7
8
9 bursting neurons or pacemaker activity plays no obligatory role in the generation of a
10
11 given rhythmic activity. Prominent examples are the generation of the respiratory rhythm
12
13 (Del Negro et al. 2005), the slow neocortical oscillations that might underlie sleep
14
15 (Sanchez-Vives and McCormick 2000), and the slow oscillations generated in the
16
17 hippocampus (Staley et al. 2001), all of which are believed to be primarily the result of
18
19 emergent network (i.e., synaptic) properties.
20
21

22
23 In the present study we examined the role of bursting neurons in neocortical
24
25 networks by selectively blocking persistent sodium currents of pyramidal neurons in
26
27 brain slices obtained from the neocortex of neonatal mice (P8-13), while observing
28
29 whether this blockade affects the generation of spontaneously generated slow network
30
31 oscillations (0.1–1 Hz). The spontaneously active isolated neocortical network enabled us
32
33 to pharmacologically manipulate cellular and network properties, a process that is more
34
35 difficult under in vivo conditions. Our data suggests that blockade of persistent sodium
36
37 currents with low concentrations of TTX and riluzole simultaneously reduces bursting
38
39 activity of intrinsically bursting pyramidal neurons and spontaneous bursting of
40
41 neocortical networks. This effect occurs without any obvious effect on postsynaptic
42
43 mechanisms. In voltage clamp studies we showed that low concentrations of TTX or
44
45 riluzole reduce the voltage-gated persistent sodium (Na_p) current. Further, in a combined
46
47 experimental and modeling approach, we confirmed that reduction of the Na_p current is
48
49 associated with a block of cellular and population bursting activity. Overall our findings
50
51 support the hypothesis that the persistent sodium current and intrinsically bursting
52
53
54
55
56
57
58
59
60

BURSTING ACTIVITY IN NEOCORTICAL NETWORKS

neurons play a critical role in the generation of rhythmic bursting behavior of neocortical networks.

METHODS

Model

The purpose of the computational approach in this study was to explain the relationship between persistent sodium conductivity and emergent network bursting behavior. The neural network in the computational model representing neocortex includes excitatory and inhibitory cell populations with a multicompartmental representation of each cell type. The network connectivity is based on histological and physiological work (DeFelipe et al. 2002; Mountcastle 1997; Nieuwenhuys 1994; Hellwig 2000; Feldmeyer and Sakman 2000; Krimer and Goldman-Rakic 2001), and includes the essence of neocortical microcircuitry.

- (1) A large fraction of excitatory cell types relative to inhibitory interneurons (a ratio of ~4:1).
- (2) Excitatory connectivity ending on the dendritic portion, while important components of the inhibition are located on the initial segment, soma, and dendrite (DeFelipe et al. 2002).
- (3) Recurrent excitation and reciprocal connection between inhibitory cells. A unique neocortical feature is the presence of axo-axonic interneurons (the chandelier cells) that do not make synaptic interconnections between themselves (DeFelipe et al. 2002; Somogyi et al. 1998).
- (4) Direct electrical contact between inhibitory interneurons (Amitai et al. 2002).

BURSTING ACTIVITY IN NEOCORTICAL NETWORKS

1
2
3 The spatiotemporal relationship between the neuronal elements is determined by the
4 geometry of the network, that is, realistic cell dimensions and spacing, associated with
5 realistic conduction speeds. Details of the model were published previously (Van
6 Drongelen et al. 2004, 2005); further parameters are summarized in the Appendix.
7
8
9

10
11
12 In short, the excitatory network (Fig. 1A) consists of superficial pyramidal cells
13 from layers 2/3 (5 compartments, Table 1) and deep pyramidal cells from layers 5/6 (7
14 compartments, Table 1). The inhibitory cells (I, Fig. 1A) receive input from both types of
15 pyramidal neurons. Gap junctions (R, Fig. 1A) between inhibitory cells show nearest
16 neighbor connectivity (e.g., Amitai et al. 2002). The implemented inhibitory interneurons
17 are three types of basket cells and the chandelier cell (B, C, respectively, in Fig. 1B). The
18 basket cell types inhibit the pyramidal cell soma, whereas the chandelier cell directly
19 inhibits the initial segment (Fig. 1B). The neurons are placed in a 3D grid and connected
20 to each other with connectivity rules derived from connections in the mammalian cortex.
21
22 In a short range, the synaptic connectivity decreases with distance between source and
23 target elements (e.g., Hellwig 2000; Feldmeyer and Sakman 2000; Krimer and Goldman-
24 Rakic 2001; Nieuwenhuys 1994). Excitatory synaptic connections were simulated by an
25 alpha function with a time constant of 1–3 ms for excitatory connectivity; inhibitory
26 synaptic activity was represented by a dual exponential function with time constants of 1
27 ms and 7 ms.
28
29
30
31
32
33
34
35
36
37
38
39
40
41
42
43
44
45
46
47

48 For fast sodium and potassium currents, implemented on the soma and initial
49 segment of the model cells, we used conductivity parameters from Hodgkin and Huxley
50 (1952); these values are justified because the parameters reported in several modeling
51 studies of cortical neurons differ only slightly with respect to activation and inactivation
52
53
54
55
56
57
58
59
60

BURSTING ACTIVITY IN NEOCORTICAL NETWORKS

1
2
3 coefficients and associated time constants (Destexhe and Pare 1999; Fleidervish and
4
5 Gutnick 1996; Golomb and Amitai 1997; Traub et al. 1994). Dynamics of the persistent
6
7 sodium channels located on the soma of a subset of the superficial pyramidal cells reflect
8
9 the measurements reported in this study.
10
11

12
13 The computational model is implemented in the parallel GENESIS model (Bower
14
15 and Beeman 1998) to facilitate a high degree of detail, large-scale simulations, and
16
17 multiple parameter searches. A scalable version of the model runs on the Jazz computing
18
19 cluster (Argonne National Laboratory), which enabled us to perform large sets of
20
21 parameter searches within a reasonable time period. Neuronal parameters were
22
23 determined with a brute force parameter search (see the Appendix) in which intrinsic and
24
25 evoked cellular behaviors were used as a target. A subsequent brute force parameter
26
27 search was used to determine network behavior. The compartmental and cellular activity
28
29 consists of complete knowledge of the local membrane potential and current. The
30
31 extracellular activity was obtained as a weighted sum of currents generated by the model
32
33 neurons (Nunez 1981).
34
35
36
37
38
39
40

Neocortical Slices

41
42
43 Neonatal (P8-13) male or female CD-1 mice (n =105) were deeply anesthetized
44
45 and decapitated at the C3/C4 spinal level, and the forebrain was isolated in ice-cold
46
47 artificial cerebrospinal fluid (ACSF). One hemisphere was then glued onto an agar block
48
49 with its rostral end up and mounted onto a vibrating tissue slicer. Coronal slices (500 μm
50
51 for current clamp and 350 μm for voltage clamp experiments) of the somatosensory
52
53 cortex were transferred into a recording chamber and submerged under a stream of ACSF
54
55
56
57
58
59
60

BURSTING ACTIVITY IN NEOCORTICAL NETWORKS

(temperature, 30°C; flow rate, 10 ml/min) containing (in mM) 118 NaCl, 3 KCl, 1.5 CaCl₂, 1 MgSO₄, 25 NaHCO₃, 1 NaH₂PO₄, and 30 D-glucose equilibrated with carbogen (95% O₂-5% CO₂). In all current clamp and extracellular experiments, the potassium concentration was routinely raised from 3 to 5 mM over 30 min to obtain spontaneous rhythmic activity close to 0.1 Hz.

Extracellular and Intracellular Current Clamp Recording

In order to obtain a signal containing multiunit action potential (AP) activity, extracellular signals were amplified 10,000 times and filtered between 0.25 and 1.5 kHz (Fig. 2B, lower trace). This signal was rectified and integrated by using an electronic integrator with a time constant of 50 ms. By applying this procedure we obtained an index for multiunit AP activity (Fig. 2B upper trace).

Intracellular current-clamp recordings were obtained from cortical neurons with the blind-patch technique. The patch electrodes were manufactured from filamented borosilicate glass tubes (Clarke GC 150TF), filled with a solution containing (in mM/l): 140 K-gluconic acid, 1 CaCl₂*6H₂O, 10 EGTA, 2 MgCl₂*6H₂O, 4 Na₂ATP, and 10 HEPES. The intracellular pipettes contained biocytin (4.5 mg/ml) to allow for identification of neuron location and morphology. Electrodes with a positive pressure of 35-50 mm Hg were penetrated deep into the slice in 10 μm steps by using a piezo-driven micromanipulator (Böhm, Germany). As the electrode approaches the cell, the measured electrode resistance increased. To obtain a Giga seal, we removed the positive pressure and applied negative suction. Recordings were low-pass filtered (0-2 kHz, Bessel 4-pole filter, -3dB) (Fig. 2C). Because the extracellular and intracellular electrodes were in close

BURSTING ACTIVITY IN NEOCORTICAL NETWORKS

1
2
3 proximity to each other (within 150 μm), the extracellular signal was used as an index for
4
5 the activity of the surrounding population (network) of neurons. After recording, the
6
7 slices were placed in a paraformaldehyde solution for subsequent staining procedures.
8
9

Voltage Clamp Recordings

10
11
12 Pyramidal neurons in layer 5 of the cortex were visually identified (ZEISS
13
14 Axioskop 2 FS microscope with IR-DIC). Whole-cell patch-clamp recordings (Fig. 2D)
15
16 were obtained with a sample frequency of 10 kHz and a low-pass filter setting of 2 kHz.
17
18 Recordings were made with unpolished patch electrodes, manufactured from borosilicate
19
20 glass pipettes with filament (Warner Instruments G150F-4). The electrodes had a
21
22 resistance of 3-5 M Ω when filled with the whole-cell patch clamp pipette solution
23
24 containing (in mM) 110 CsCl, 30 TEA-Cl, 1 CaCl₂, 10 EGTA, 2 MgCl₂, 4 Na₂ATP,
25
26 10 HEPES (pH 7.2). The patch-clamp experiments were performed with a patch-clamp
27
28 amplifier (AxoPatch 200B), a digitizing interface (Digidata 1322A), and the software
29
30 program pClamp 9.2 (Axon Instruments).
31
32
33
34
35
36
37
38

39
40 Neurons located at least three to four cell layers (approx. 80–150 μm) caudal from
41
42 the rostral surface of the slice were recorded under visual control (inset, Fig. 3A).
43
44 Neurons located directly at the slice surface were not examined because they were more
45
46 likely to be damaged during the preparation than were neurons located deeper within the
47
48 slice. Current response traces were recorded with either off- or online leak subtraction
49
50 (P/4 protocol), eliminating the linear leak current and residual capacity currents. The
51
52 liquid junction potential was 2 mV and was manually subtracted with the amplifier's
53
54 pipette offset regulator immediately before establishing the patch clamp configuration.
55
56
57
58
59
60

BURSTING ACTIVITY IN NEOCORTICAL NETWORKS

1
2
3 The series resistance was always 80% compensated and regularly corrected throughout
4 the experiments. We emphasize that whole-cell voltage clamp recordings from neurons
5 embedded in a functional network are accompanied by difficult space clamp control. This
6 could lead to incorrect values for current amplitudes. Thus, recordings with obvious
7 space clamp problems (Armstrong and Gilly 1992) were discarded. Poor space clamping
8 was indicated by rebound spikes (rapid, fast inactivating inward currents, which were
9 induced by steps from depolarizing test potentials to the former holding potential) or an
10 increase in the delay to onset of an inward current with increasing magnitude of test
11 pulse. Steps to higher test potentials were typically associated with a reduction in delay to
12 current onset. We also discarded neurons with insufficiently blocked K^+ currents, evident
13 in outward currents typically commencing at voltage steps to 10 mV.
14
15
16
17
18
19
20
21
22
23
24
25
26
27
28

29 Using the conventional patch-clamp technique, we pharmacologically isolated
30 both the voltage-activated calcium and the voltage-activated sodium currents by
31 intracellular blockade of voltage-activated potassium currents with 110 mM CsCl and 30
32 mM tetraethylammonium (TEA) chloride. As shown in a previous study (Elsen and
33 Ramirez 1998), this blockade was sufficient for the investigation of the maximal inward
34 current amplitude. In addition, voltage-activated calcium currents were blocked by extra
35 cellular bath application of 200 μ M cadmium chloride ($CdCl_2$) to isolate the persistent
36 sodium current.
37
38
39
40
41
42
43
44
45
46
47
48
49
50

Synaptic Input Measurements

51
52 To examine potential postsynaptic effects of riluzole at a concentration of 20 μ M,
53 we eliminated action potential evoked synaptic events and added 1 μ M tetrodotoxin
54
55
56
57
58
59
60

BURSTING ACTIVITY IN NEOCORTICAL NETWORKS

(TTX) to the ACSF. Miniature excitatory and inhibitory postsynaptic currents (mEPSCs and mIPSCs, respectively) were recorded and digitized for a period of 4 minutes per data file. Signals were sampled with a frequency of 10 kHz (filtered with 2 kHz) at a holding potential (V_h) of -60 mV and stored for subsequent analysis. The recording electrodes had a resistance of 3–5 M Ω when filled with the whole-cell patch clamp pipette solution containing (in mM) 138 Cs-Me-sulfonate, 2 NaCl, 1 CaCl₂, 10 EGTA, 4 Na₂ATP, 0.3 Na-GTP, and 10 HEPES (pH 7.2). Consulting equilibrium potential to holding potential relationships, all upward deflections had to be chloride-conducting, inhibitory currents, whereas all downward deflection had to be miniature excitatory postsynaptic currents.

To ensure steady drug (riluzole) concentration equilibrium in the recording chamber, a 4-minute preapplication of riluzole-containing solution was carried out before the start of the actual 4-minute data recording that was used for the later analysis.

Experiments

Both network activity and cellular activity were studied after a rhythmically active slice was obtained (Fig. 2B, C). To investigate the role of the persistent sodium current (I_{Na_p}), in the generation of network bursting and cellular activity, we applied either riluzole (20 μ M) or a very low concentration TTX (50 nM) to the ACSF. In some of the experiments, the neurons were decoupled from the network by blocking non-NMDA and NMDA glutamatergic receptors using CNQX (20 μ M) and CPP (10 μ M); adding this combination of drugs in the ACSF stopped network activity within a few minutes.

BURSTING ACTIVITY IN NEOCORTICAL NETWORKS

To explore the effectiveness of riluzole and a low concentration of TTX and the role of persistent sodium in cellular and network activity, we carried out the following experiments.

1. By means of the voltage clamp technique, the persistent sodium conductivity before and after addition of riluzole (n=5) or a low concentration of TTX (n=7) was determined in pyramidal neurons after they were isolated from the network.
2. In five experiments we also determined the effect of riluzole on calcium currents in the presence of TTX (1 μ M).
3. The effect of riluzole on postsynaptic activity was recorded in voltage clamp mode (n=9).
4. The neuronal response to current injection (50–150 pA) was determined before and after bath application of riluzole (n= 12) or low concentration TTX (n=8) and every 30 seconds thereafter for 10 minutes. Responses of RS type neurons were evaluated only during absence of overt network activity. The IB type neurons were isolated from the network to confirm that the bursting was intrinsic and not network driven. The response evoked by the current injection was quantified by the number of action potentials in one second following onset of injection.
5. Riluzole (n=13) or TTX (n=8) was added to the ACSF, and network bursting activity was observed and quantified for 10 minutes after drug application.

The extracellular and intracellular current clamp recordings were performed in a different setup from that for the voltage clamp measurements. Because of differences in the tubing of each setup, there was a 60-second difference in latency between drug delivery to the

BURSTING ACTIVITY IN NEOCORTICAL NETWORKS

1
2
3 ACSF system and arrival in the bath. The drug delivery difference is compensated for in
4
5
6 the graphs of Fig. 7 by shifting the graphs relative to each other.
7
8
9

Data Analysis

10
11
12 Data were analyzed by using MiniAnalysis 5.41 (Synaptosoft), and statistical
13
14 analysis was performed with Prism 4.03 (Graphpad). Significance between data values
15
16 was assessed with the student's t-test and assumed when $p \leq .05$. Voltage clamp data
17
18 were analyzed off-line with the software program ClampFit 9.2 (Axon Instruments).
19
20
21
22 Quantitative data is given as mean \pm standard error.
23
24

25
26 A computerized preanalysis of each 4-minute recording was performed to tag all
27
28 events that qualified as miniature excitatory postsynaptic currents (mEPSCs) according to
29
30 the user-defined, program-specific detection parameters. However, an additional manual
31
32 user-performed screen through each data trace was necessary to eliminate computer
33
34 errors. During this eyeballed-screening process, wrongly tagged artificial events were
35
36 unmarked, and missed real mEPSC events were tagged. In order to determine the
37
38 representative amplitude and decay time of the recorded mEPSCs in each data trace, an
39
40 average mEPSC from 50 single mEPSCs was created as follows: For each 4-minute data
41
42 trace, the computer randomly picked 75 single events. Those events were superimposed
43
44 and aligned at 50% rise time. Manual eyeballed control was used to eliminate single
45
46 events that did not line up within a rise-time window of 4 ms. In addition, the decay
47
48 phase of each event had to steadily decay without any interruption by additional events or
49
50 noise for 50 ms. This procedure was followed until 50 events were included into the
51
52
53
54
55
56
57
58
59
60
61
62
63
64
65
66
67
68
69
70
71
72
73
74
75
76
77
78
79
80
81
82
83
84
85
86
87
88
89
90
91
92
93
94
95
96
97
98
99
100
101
102
103
104
105
106
107
108
109
110
111
112
113
114
115
116
117
118
119
120
121
122
123
124
125
126
127
128
129
130
131
132
133
134
135
136
137
138
139
140
141
142
143
144
145
146
147
148
149
150
151
152
153
154
155
156
157
158
159
160
161
162
163
164
165
166
167
168
169
170
171
172
173
174
175
176
177
178
179
180
181
182
183
184
185
186
187
188
189
190
191
192
193
194
195
196
197
198
199
200
201
202
203
204
205
206
207
208
209
210
211
212
213
214
215
216
217
218
219
220
221
222
223
224
225
226
227
228
229
230
231
232
233
234
235
236
237
238
239
240
241
242
243
244
245
246
247
248
249
250
251
252
253
254
255
256
257
258
259
260
261
262
263
264
265
266
267
268
269
270
271
272
273
274
275
276
277
278
279
280
281
282
283
284
285
286
287
288
289
290
291
292
293
294
295
296
297
298
299
300
301
302
303
304
305
306
307
308
309
310
311
312
313
314
315
316
317
318
319
320
321
322
323
324
325
326
327
328
329
330
331
332
333
334
335
336
337
338
339
340
341
342
343
344
345
346
347
348
349
350
351
352
353
354
355
356
357
358
359
360
361
362
363
364
365
366
367
368
369
370
371
372
373
374
375
376
377
378
379
380
381
382
383
384
385
386
387
388
389
390
391
392
393
394
395
396
397
398
399
400
401
402
403
404
405
406
407
408
409
410
411
412
413
414
415
416
417
418
419
420
421
422
423
424
425
426
427
428
429
430
431
432
433
434
435
436
437
438
439
440
441
442
443
444
445
446
447
448
449
450
451
452
453
454
455
456
457
458
459
460
461
462
463
464
465
466
467
468
469
470
471
472
473
474
475
476
477
478
479
480
481
482
483
484
485
486
487
488
489
490
491
492
493
494
495
496
497
498
499
500
501
502
503
504
505
506
507
508
509
510
511
512
513
514
515
516
517
518
519
520
521
522
523
524
525
526
527
528
529
530
531
532
533
534
535
536
537
538
539
540
541
542
543
544
545
546
547
548
549
550
551
552
553
554
555
556
557
558
559
560
561
562
563
564
565
566
567
568
569
570
571
572
573
574
575
576
577
578
579
580
581
582
583
584
585
586
587
588
589
590
591
592
593
594
595
596
597
598
599
600
601
602
603
604
605
606
607
608
609
610
611
612
613
614
615
616
617
618
619
620
621
622
623
624
625
626
627
628
629
630
631
632
633
634
635
636
637
638
639
640
641
642
643
644
645
646
647
648
649
650
651
652
653
654
655
656
657
658
659
660
661
662
663
664
665
666
667
668
669
670
671
672
673
674
675
676
677
678
679
680
681
682
683
684
685
686
687
688
689
690
691
692
693
694
695
696
697
698
699
700
701
702
703
704
705
706
707
708
709
710
711
712
713
714
715
716
717
718
719
720
721
722
723
724
725
726
727
728
729
730
731
732
733
734
735
736
737
738
739
740
741
742
743
744
745
746
747
748
749
750
751
752
753
754
755
756
757
758
759
760
761
762
763
764
765
766
767
768
769
770
771
772
773
774
775
776
777
778
779
780
781
782
783
784
785
786
787
788
789
790
791
792
793
794
795
796
797
798
799
800
801
802
803
804
805
806
807
808
809
810
811
812
813
814
815
816
817
818
819
820
821
822
823
824
825
826
827
828
829
830
831
832
833
834
835
836
837
838
839
840
841
842
843
844
845
846
847
848
849
850
851
852
853
854
855
856
857
858
859
860
861
862
863
864
865
866
867
868
869
870
871
872
873
874
875
876
877
878
879
880
881
882
883
884
885
886
887
888
889
890
891
892
893
894
895
896
897
898
899
900
901
902
903
904
905
906
907
908
909
910
911
912
913
914
915
916
917
918
919
920
921
922
923
924
925
926
927
928
929
930
931
932
933
934
935
936
937
938
939
940
941
942
943
944
945
946
947
948
949
950
951
952
953
954
955
956
957
958
959
960
961
962
963
964
965
966
967
968
969
970
971
972
973
974
975
976
977
978
979
980
981
982
983
984
985
986
987
988
989
990
991
992
993
994
995
996
997
998
999
1000

BURSTING ACTIVITY IN NEOCORTICAL NETWORKS

1
2
3 average mEPSC (Fig. 4B) delivered a representative amplitude and decay time constant
4
5
6 (τ). This analysis was not performed on the inhibitory component, due to a low frequency
7
8 of occurrence of mIPSCs before and after adding riluzole.
9

10 11 12 RESULTS

13 14 *Voltage Clamp Data*

15
16 We recorded in the voltage-clamp mode from 51 neurons in layer 5 of the
17
18 neocortex. The average cell capacity was 107 ± 14 pF, and cell resistance was 365 ± 92
19
20 M Ω . After blockade of voltage-activated calcium (bath: 200 μ M CdCl₂) and potassium
21
22 (intracellular: 110 mM CsCl, 30 mM TEA-Cl) currents, we evoked voltage-activated
23
24 persistent sodium currents (I_{NaP}) with specific voltage step protocols (Fig. 3A, C insets).
25
26 The I_{NaP} amplitudes were measured at the steady-state level toward the end of the voltage
27
28 steps (● in Fig. 3A) and were plotted against the respective test potentials (average I/V-
29
30 curve, Fig. 3B). The peak voltage range of the I_{NaP} currents were between -30 and
31
32 -10mV, with a maximum amplitude between 307 ± 33 and 333 ± 34 pA.
33
34
35
36
37
38

39
40 To determine the activation properties, we calculated the I_{NaP} conductance (g) to
41
42 compensate for the changing driving force at respective test potentials ($g = I/V_t - E_q$, with V_t
43
44 as test potential and E_q as equilibrium potential). The I_{NaP} conductance values were
45
46 normalized, and the average was plotted against the respective test potentials (Fig. 3F). A
47
48 sigmoidal Boltzman-curve fit $1/(1 + e^{-(V-V_{50})/slope})$ for the normalized I_{NaP} amplitudes as a
49
50 function of the test potential V delivered the activation parameters: $V_{50} = -46.2 \pm 1.4$ mV
51
52 and slope = 9.9 ± 1.3 . Both low TTX and riluzole significantly reduced the I_{NaP} current
53
54 (Fig. 3B) and resulted in a lower level of activation (Fig. 3F).
55
56
57
58
59
60

BURSTING ACTIVITY IN NEOCORTICAL NETWORKS

To determine the inactivation properties of the I_{NaP} currents, we measured the I_{NaP} current amplitudes at the peak voltage (-15 mV) immediately after different prolonged (10 s) test potentials (Fig. 3D). The remaining, activatable I_{NaP} amplitudes were normalized (I/I_{max}), and the average was plotted against the respective test potentials (Fig. 3E). A sigmoidal Boltzman-fit delivered the inactivation parameters: $V_{50} = -65.4 \pm 2.3$ mV and slope = -19.0 ± 2.5 . No significant effects of riluzole on Ca^{2+} currents were measured ($n=5$).

Synaptic Properties

To investigate possible postsynaptic effects of riluzole, we compared miniature excitatory postsynaptic currents (mEPSCs) under control conditions (with TTX (1 μ M) to disable spike activity) with mEPSCs after additional application of 20 μ M riluzole (Fig. 4). The difference of the frequency of mEPSCs, 0.9 ± 0.5 Hz under control conditions and 1.3 ± 0.6 Hz after adding riluzole, was not significant. For the mIPSCs the frequency was very low both under control conditions (0.05 Hz) and after adding riluzole (0.04 Hz). In five cells using 50 single events of a 4-minute recording for each neuron, we found that neither the mEPSC amplitudes (TTX: 19.8 ± 1.1 pA, TTX+riluzole: 20.4 ± 1.2 pA), nor the mEPSC decay time constants (TTX: 4.6 ± 0.4 ms, TTX+riluzole: 4.2 ± 0.2 ms) were significantly different from each other (Fig. 4B, C). Because of these low numbers for the inhibitory events, a meaningful averaging procedure and subsequent quantitative analysis was not feasible.

Cellular Activity

BURSTING ACTIVITY IN NEOCORTICAL NETWORKS

1
2
3
4
5
6
7
8
9
10
11
12
13
14
15
16
17
18
19
20
21
22
23
24
25
26
27
28
29
30
31
32
33
34
35
36
37
38
39
40
41
42
43
44
45
46
47
48
49
50
51
52
53
54
55
56
57
58
59
60

In the presence of 5 mM of $[K^+]$, stable baseline bursting activity is generated at the network level (Van Drongelen et al. 2003a). Simultaneous extracellular recordings from population bursts and intracellular recordings from individual neurons revealed that all neurons were either excited or inhibited in phase with population activity; that is, neurons received synaptic inputs from the network. Typical patterns (Van Drongelen et al. 2003a) were excitation, excitation followed by inhibition, and inhibition as shown for RS type cells in Fig. 5A and for IB type neurons in Fig. 5B.

The persistent sodium current is involved in the control of intrinsic excitability of neocortical pyramidal neurons; however, the effect depended on cell type (Fig. 6). Examples of the effect of riluzole on regular spiking and intrinsically bursting cells are shown in Fig. 6A. When network bursting stopped, the RS type neurons were not significantly affected by riluzole ($n=8$, $p=0.26$) (Fig. 5C1, D1); the average number of AP/s was 10.7 ± 0.8 before and 9.4 ± 1.3 after riluzole application. However, 10 minutes after network cessation, the neural response evoked by current injection into RS neurons became significantly reduced ($p < .05$, 3.0 ± 1.2 AP/s). By contrast, bursting activity in intrinsically bursting neurons (IB) completely disappeared and became regular spiking within 5-6 minutes after riluzole application (Fig. 6A2, A3, B2). As a consequence of the loss of bursts the number of action potentials generated by the current injection was significantly ($p < .05$) decreased ($n=4$: AP/s 9.2 ± 1.0 before adding riluzole and 4.4 ± 0.8 after the application of riluzole, Fig. 6C2). The difference between activity levels of the RS and IB type neurons under control conditions was not significant, but activity levels of IB neurons were significantly reduced in the presence of riluzole. The time course of

BURSTING ACTIVITY IN NEOCORTICAL NETWORKS

1
2
3 the activity levels of both RS and IB type neurons in the presence of riluzole is depicted
4
5
6 in Fig. 7B.

7
8 To address the possibility that these results were caused by the known unspecific
9
10 effects of riluzole, we repeated these experiments with TTX at low concentrations. The
11
12 response in RS type neurons (n=4) was not significantly affected (p=.55) within 5–6
13
14 minutes of bath-applied TTX. By contrast, the bursting in IB type neurons was blocked
15
16 within 5–6 minutes, significantly decreasing the frequency of action potentials (n=4:
17
18 p<.01, AP/s 11.1 ±2.8 before adding TTX and 4.7 ± 2.2 after the network stopped
19
20 bursting). The time course of the activity levels of both RS and IB type neurons is
21
22 depicted in Fig. 7E.
23
24
25
26
27
28

29 *Network Activity*

30
31 In order to obtain stable baseline bursting activity of 0.234 ± 0.08 Hz, 5 mM of $[K^+]$ was
32
33 used. Network activity expressed in bursts per second decreased drastically after adding
34
35 20 μ M riluzole (n=13) or 50 nM TTX (n=5) to the bath (Fig. 7 A, D). In both cases there
36
37 was a 100 s latency between adding the drug and a reduction in the burst activity level.
38
39 All network bursting activity in the slice disappeared after 280.0 ± 49.0 s after
40
41 administration of 50 nM TTX and 403.8 ± 40.2 s after 20 μ M riluzole was added to the
42
43 ACSF. The overall reduction in network bursting 10 minutes after bath application of
44
45 both drugs was significant (p <.01).
46
47
48
49
50
51
52
53
54
55
56
57
58
59
60

54 *Simulated Activity*

BURSTING ACTIVITY IN NEOCORTICAL NETWORKS

1
2
3 Although we found that the Na_p current is not strictly a persistent current because
4 it does inactivate, its voltage clamp characteristic shows a fairly large window in which
5 these channels can be activated (Fig. 3E). This property indicates that a small,
6
7
8 “persistent” sodium current is present during the resting state of the neurons, causing the
9 membrane to slowly depolarize up to the threshold for generating action potentials. This
10 small depolarizing current causes neurons to burst at regular intervals. At small offset
11 depolarization (or current injections) the neurons burst more frequently, whereas at
12 higher levels of depolarization the neurons show beating (continuous spiking) behavior
13 identical to the activity pattern described by Butera et al. (1999). The computational
14 model included bursting and RS type pyramidal neurons (Fig. 8A-D) and interneurons
15 that fired at higher rates and lower thresholds (Fig. 8E-H).
16
17
18
19
20
21
22
23
24
25
26
27
28

29 The model network that included the bursting pyramidal cell type (Fig. 8A)
30 immediately settled into a pattern of bursting network activity (Fig. 8I). In the absence of
31 the Na_p channels in this cell type, network bursts were absent as well. The trace shown in
32 Fig. 8I was obtained by reducing the maximum conductance of Na_p from 65 to 0.065
33 S/m² over a time interval of 12 min. This decrease was done in a logarithmic fashion to
34 mimic the penetration of riluzole into the slice. By following this procedure we gradually
35 attenuated the effect of Na_p current similar to the riluzole or TTX experiments shown in
36 Fig. 7. A typical example of a recorded trace from a slice is shown in Fig. 8J; in this
37 experiment riluzole was used to attenuate bursting activity. It can be seen that network
38 activity initially decreases and stops within 10 min, both in the simulated and recorded
39 traces in Fig. 7I and Fig. 7J, respectively.
40
41
42
43
44
45
46
47
48
49
50
51
52
53
54
55
56
57
58
59
60

BURSTING ACTIVITY IN NEOCORTICAL NETWORKS

DISCUSSION

Our data suggests that persistent sodium current is important both for the generation of bursting activity in a subset of neocortical neurons and for the generation of bursting at the network level. In the presence of low concentrations of TTX or the neuroprotective drug riluzole, the spontaneous network bursting activity in neocortical slices of neonatal mice was suppressed (Fig. 7A, D). To our knowledge this is the first study in which the role of riluzole is quantified and modeled at the level of

- (1) intrinsic (persistent sodium) membrane currents (Fig. 3),
- (2) single neuron activity (Figs. 6 and 7), and
- (3) network activity (Fig. 7).

Although we emphasize that our modeling was not an exact fitting procedure to the recorded data, the experimental findings were essentially confirmed in the computational model (Fig. 8).

Our study also confirmed previous experimental and computational studies that indicate that the Na_p conductance plays a major role in providing intrinsic excitation to cortical networks (Agrawal et al. 2001; Bazhenov et al. 2002, 2004). Combined in vivo recordings and computational models indicate that the interplay between the hyperpolarization-activated depolarizing current (I_H), Ca^{++} -sensitive potassium current, and a persistent sodium current could organize paroxysmal oscillations (Timofeev et al. 2000). The persistent sodium current plays an important role in activating intrinsic bursting in neocortical neurons (Guatteo et al. 1996), and a number of studies have demonstrated that the number of intrinsically bursting neurons is significantly increased after neocortical trauma or conditions that enhance the propensity of epilepsy (Sanabria et

BURSTING ACTIVITY IN NEOCORTICAL NETWORKS

1
2
3 al. 2002; Topolnik et al. 2003). Steriade and coworkers have demonstrated that
4
5 intrinsically bursting neurons are frequently found in vivo (20–25% of the total cortical
6
7 neuronal population), and these authors have proposed that these bursting neurons play a
8
9 critical role in the generation of seizure activity (Timofeev et al. 2000; Timofeev and
10
11 Steriade 2004). Indeed, intrinsically bursting neurons are rhythmically active during
12
13 Lennox-Gastaut-type seizures, specifically during spike wave (SW) discharges, polyspike
14
15 wave (PSW) complexes, and fast runs (Timofeev and Steriade 2004). Mechanistically,
16
17 bursting in these neurons could have a large impact on local networks that initiate
18
19 seizures focally and in related structures as proposed by Steriade and co-workers
20
21 (Steriade et al. 1998; Timofeev and Steriade 2004). Such neurons could also play a role
22
23 in triggering ripples that in turn would facilitate seizure generation, not only in the
24
25 neocortex, but also in the hippocampus (Bragin et al. 1999a, 1999b, 1999c, 2002; Fisher
26
27 et al. 1992; Grenier et al. 2001; Timofeev and Steriade 2004; Traub et al. 2001). The
28
29 cellular bursting property together with a modest level of synchrony and recurrent
30
31 excitation can lead to a seizure-like pattern (Van Drongelen et al. 2003a, 2005). Our
32
33 current result suggesting that intrinsic cellular bursting properties associated with the
34
35 persistent sodium current are a critical component of synchronous activity in cortical
36
37 neuronal populations agrees well with the reported anticonvulsant action of persistent
38
39 sodium blockers in some patients with epilepsy (Köhling 2002).
40
41
42
43
44
45
46
47

48 In addition to the potential role of Na_p in epilepsy, the bursting properties
49
50 associated with this persistent current may very well drive physiological oscillations
51
52 observed in sleep and memory formation (e.g., Agrawal et al. 2001; Bazhenov et al.
53
54 2002; Timofeev et al. 2000). The rhythmic network bursting as described in the present
55
56
57
58
59
60

BURSTING ACTIVITY IN NEOCORTICAL NETWORKS

1
2
3 study could represent an in vitro form of slow sleep oscillation. Such oscillations are
4
5 known to develop into SW/PSW seizures in vivo (Steriade and Amzica 2003; Timofeev
6
7 and Steriade 2004). We emphasize, however, that in a functional network, the persistent
8
9 sodium channels not only function in form of intrinsic bursting but also could amplify
10
11 currents flowing through glutamate-activated dendritic channels (Crill 1999; Schwindt
12
13 and Crill 1999; Timofeev et al. 2000). The involvement of the persistent sodium current
14
15 in the generation of intrinsic bursting could also explain the finding that the propensity to
16
17 burst is a “flexible” property (Steriade 2004). The persistent sodium current and bursting
18
19 neurons are a target of various neuromodulators (Peña and Ramirez 2002; Staiger et al.
20
21 2002).

22
23
24
25
26
27 From a theoretical point of view, network bursting activity can be caused by
28
29 cellular oscillations due to intrinsic membrane conductance, network properties, or a
30
31 combination of both. Current modeling results and earlier simulation studies demonstrate
32
33 that networks of RS type pyramidal cells can oscillate at an appropriate combination and
34
35 strength of connectivity but that intrinsic bursting neuronal activity is critical for
36
37 sustaining slow bursting network activity (Traub et al. 2003; Van Drongelen et al. 2004,
38
39 2005). In our study, low concentrations of TTX or riluzole inhibited the persistent sodium
40
41 current (Fig. 3), while leaving postsynaptic function intact (Fig. 4). At the cellular level,
42
43 we found that reducing the persistent sodium current through low TTX or riluzole can
44
45 change the firing properties of IB neurons dramatically (Fig. 6). The bursting behavior of
46
47 these neurons was altered, and they converted to a pattern similar to regular firing, with a
48
49 reduced output of action potentials per injected current pulse (Fig 6C2). Similar
50
51 experiments with regular firing (RS type) neurons showed that their firing pattern was
52
53
54
55
56
57
58
59
60

BURSTING ACTIVITY IN NEOCORTICAL NETWORKS

1
2
3 unchanged at the cessation of network bursting (Figs. 6C1, 7B, E). However, current
4
5
6 injections 10 min or more after cessation of network bursting showed that all cell types
7
8 had a significantly decreased activity level. Our findings suggest that the persistent
9
10 sodium current plays a role in enhancing excitability of the majority of neocortical
11
12 neurons but that the intrinsic bursting property is more sensitive to the blockade of Na_p
13
14 than the generation of regular spiking activity. Such a differential sensitivity could
15
16 explain why intrinsic bursting was blocked first. However, we have not attempted to
17
18 investigate the reason for the observed differential effect; the focus of the present study
19
20 was to use this differential effect as a pharmacological tool to determine factors involved
21
22 in reducing network activity that finally leads to the cessation of network bursting.
23
24
25
26

27 The computational approach confirmed the essence of our experimental
28
29 observation and showed that Na_p caused periodic bursting at the cellular level (Fig. 8A),
30
31 identical to the pattern reported in Butera et al. (1999). At the network level this feature
32
33 was associated with a bursting pattern, although without the simple periodicity (Fig. 8I).
34
35 This finding together with the absence of network bursting at attenuated Na_p currents
36
37 suggests that the bursting neurons in a network recruit surrounding neurons at irregular
38
39 intervals. In this state of the network the neurons are not acting as simple pacemakers that
40
41 synchronize other units into their intrinsic periodic rhythm; rather, they function merely
42
43 as units that occasionally can drive or recruit a critical mass of neurons resulting in a
44
45 burst of activity, while the network in its turn codetermines the state of these bursters—
46
47 clearly a bidirectional process, as similarly discussed by Ramirez et al. (2004). Therefore
48
49 we propose that the intrinsic (Na_p current) and network property (excitatory connectivity)
50
51 together sustain the rhythmic network behavior that we observed in the neocortical slices.
52
53
54
55
56
57
58
59
60

BURSTING ACTIVITY IN NEOCORTICAL NETWORKS

ACKNOWLEDGMENTS

We thank Dr. K.E. Hecox for his support. Current address of Drs. F. P. Elsen and C. J. Marcuccilli: Department of Neurology, Medical College of Wisconsin, Milwaukee, WI.

GRANTS

Part of this work was supported by a Falk Grant and by the U.S. Department of Energy under Contract W-31-109-ENG-38.

BURSTING ACTIVITY IN NEOCORTICAL NETWORKS

REFERENCES

Agrawal N, Hamam BN, Magistretti J, Alonso A, and Ragsdale DS. Persistent sodium channel activity mediates subthreshold membrane potential oscillations and low-threshold spikes in rat entorhinal cortex layer V neurons. *Neuroscience* 102: 53-64, 2001.

Amitai Y, Gibson JR, Beierlein M, Patrick SL, Ho AM, Connors BW, and Golomb D. The spatial dimensions of electrically coupled networks of interneurons in the neocortex. *J Neurosci* 22: 4142-4152, 2002.

Armstrong CM and Gilly WF. Access resistance and space clamp problems associated with whole cell patch clamping. *Methods Enzymol* 207: 100-122, 1992.

Arshavsky YI. Cellular and network properties in the functioning of the nervous system: from central pattern generators to cognition. *Brain Res Brain Res Rev* 41:229-67, 2003.

Bazhenov M, Timofeev I, Steriade M, and Sejnowski TJ. Model of thalamocortical slow-wave sleep oscillations and transitions to activated States. *J Neurosci* 22:8691-704, 2002.

Bazhenov M, Timofeev I, Steriade M, and Sejnowski TJ. Potassium model for slow (2-3 Hz) in vivo neocortical paroxysmal oscillations. *J Neurophysiol* 92:1116-32, 2004.

BURSTING ACTIVITY IN NEOCORTICAL NETWORKS

1
2
3 **Blatow M, Rozov A, Katona I, Hormuzdi SG, Meyer AH, Whittington MA, Caputi**
4 **A, and Monyer H.** A novel network of multipolar bursting interneurons generates theta
5 frequency oscillations in neocortex. *Neuron* 38:805-17, 2003.
6
7

8
9
10
11
12 **Bower JM and Beeman D.** *The Book of Genesis*. New York: Springer-Verlag, 1998.
13
14

15
16
17 **Bragin A, Engel J, Wilson CL, Fried I, and Buzsáki G.** High-frequency oscillations in
18 human brain. *Hippocampus* 9: 137–142, 1999a.
19
20

21
22
23 **Bragin A, Engel J, Wilson CL, Fried I, and Mathern GW.** Hippocampal and
24 entorhinal cortex high-frequency oscillations (100–150 Hz) in human epileptic brain and
25 in kainic acid-treated rats with chronic seizures. *Epilepsia* 40: 127–137, 1999b.
26
27
28

29
30
31 **Bragin A, Engel J, Wilson CL, Vizenin E, and Mathern GW.** Electrophysiologic
32 analysis of a chronic seizure model after unilateral hippocampal KA injection. *Epilepsia*
33 40: 1210–1221, 1999c.
34
35
36

37
38
39 **Bragin A, Modi I, Wilson CL, and Engel J.** Local generation of fast ripples in epileptic
40 brain. *J Neurosci* 22: 2012–2021, 2002.
41
42
43

44
45
46 **Bremer F.** Considerations sur l'origine et la nature des "ondes" cerebrales. *EEG Clin*
47 *Neurophysiol* 177-193, 1949.
48
49
50
51
52
53
54
55
56
57
58
59
60

BURSTING ACTIVITY IN NEOCORTICAL NETWORKS

1
2
3 **Bush PC and Sejnowski TJ.** Reduced compartmental models of neocortical pyramidal
4 cells. *J Neuroscience Methods* 46: 159-166, 1993.
5
6
7

8
9
10 **Butera RJ, Rinzel J, and Smith JC.** Models of respiratory rhythm generation in the pre-
11 Bötzing complex, I: Bursting pacemaker neurons. *J Neurophysiol* 82: 382–397, 1999.
12
13
14

15
16
17 **Connors BW and Gutnick MJ.** Intrinsic firing patterns of diverse neocortical neurons.
18 *Trends Neurosci* 13:365-6, 1990.
19
20
21

22
23
24 Crill WE. Functional implications of dendritic voltage-dependent conductances.
25
26
27 *J Physiol Paris*. 1999 Jan-Apr;93(1-2):17-21.
28
29

30
31 **Cunningham MO, Whittington MA, Bibbig A, Roopun A, LeBeau FE, Vogt A,**
32 **Monyer H, Buhl EH, and Traub RD.** A role for fast rhythmic bursting neurons in
33 cortical gamma oscillations in vitro. *Proc Natl Acad Sci* 101:7152-7157, 2004.
34
35
36
37

38
39
40 **Darbon P, Yvon C, Legrand JC, and Streit J.** INaP underlies intrinsic spiking and
41 rhythm generation in networks of cultured rat spinal cord neurons. *Eur J Neurosci*
42
43
44
45
46
47
48
49
20:976-88, 2004.

50
51 **DeFelipe J, Alonso-Nanclares L, and Arellano JI.** Microstructure of the neocortex:
52 Comparative aspects *J Neurocytol* 31: 299–316, 2002.
53
54
55
56
57
58
59
60

BURSTING ACTIVITY IN NEOCORTICAL NETWORKS

1
2
3 **Dégenétais E, Thierry A-M, Glowinski J, and Gioanni Y** Electrophysiological
4 Properties of Pyramidal Neurons in the Rat Prefrontal Cortex: An In Vivo Intracellular
5
6 Recording Study. *J Neurophysiol* 89:1541-66, 2003.
7
8
9

10
11
12 **Del Negro CA, Morgado-Valle C, Hayes JA, Mackay DD, Pace RW, Crowder EA,**
13 **and Feldman JL.** Sodium and calcium current-mediated pacemaker neurons and
14 respiratory rhythm generation. *J Neurosci.* 25:446-53, 2005.
15
16
17
18
19

20
21
22 **Destexhe A and Pare D.** Impact of network activity on the integrative properties of
23 neocortical pyramidal neurons in vivo. *J Neurophysiol* 81:1531-1547, 1999.
24
25
26
27

28
29 **Elsen FP and Ramirez JM.** Calcium currents of rhythmic neurons recorded in the
30 isolated respiratory network of neonatal mice. *J Neurosci* 18:10652-1062, 1998.
31
32
33
34

35
36 **Feldmeyer D and Sakmann B.** Synaptic efficacy and reliability of excitatory
37 connections between principle neurones of the input (layer 4) and output (layer 5) of the
38 neocortex. *J Physiol* 525: 31-39, 2000.
39
40
41
42
43

44
45
46 **Fisher RS, Webber WR, Lesser RP, Arroyo S, and Uematsu S.** High-frequency EEG
47 activity at the start of seizures. *J Clin Neurophysiol* 9: 441-448, 1992.
48
49
50
51
52
53
54
55
56
57
58
59
60

BURSTING ACTIVITY IN NEOCORTICAL NETWORKS

1
2
3 **Fleidervish IA and Gutnick MJ.** Kinetics of slow inactivation of persistent sodium
4 current in layer V neurons of mouse neocortical slices. *J Neurophysiol* 76: 2125-2130,
5
6
7
8 1996.
9

10
11
12 **Foehring RC, van Brederode JF, Kinney GA, and Spain WJ.** Serotonergic
13 modulation of supragranular neurons in rat sensorimotor cortex, *J Neurosci* 22:8238-50,
14
15
16
17 2002.
18

19
20
21 **Foehring RC and Wyler AR.** Two patterns of firing in human neocortical neurons.
22
23
24 *Neurosci Lett* 110:279-85, 1990.
25
26

27
28
29 **Golomb D and Amitai Y.** Propagating neuronal discharges in neocortical slices:
30
31
32 computational and experimental study. *J Neurophysiol* 78: 1199-1211, 1997.
33
34

35
36
37 **Gray CM and McCormick DA.** Chattering cells: superficial pyramidal neurons
38
39
40 contributing to the generation of synchronous oscillations in the visual cortex. *Science*
41
42 274:109-113, 1996.
43
44

45
46 **Grenier F, Timofeev I, and Steriade M.** Focal synchronization of ripples (80-200 Hz)
47
48
49 in neocortex and their neuronal correlates. *J Neurophysiol* 86:1884-1898, 2001.
50
51
52
53
54
55
56
57
58
59
60

BURSTING ACTIVITY IN NEOCORTICAL NETWORKS

1
2
3 **Guatteo E, Franceschetti S, Bacci A, Avanzini G, and Wanke E.** A TTX-sensitive
4 conductance underlying burst firing in isolated pyramidal neurons from rat neocortex.
5
6

7
8 *Brain Res* 741:1-12, 1996.
9

10
11
12 **Hellwig B.** A quantitative analysis of the local connectivity between pyramidal neurons
13 in layer 2/3 of the rat visual cortex. *Biol Cybern* 82: 111-121, 2000.
14
15
16

17
18
19
20 **Hodgkin AL and Huxley AF.** A quantitative description of membrane current and its
21 application to conduction and excitation in nerve. *J Physiol* 117: 500-544, 1952
22
23

24
25
26
27 **Istvan PJ and Zarzecki P.** Intrinsic discharge patterns and somatosensory inputs for
28 neurons in raccoon primary somatosensory cortex, *J Neurophysiol* 72: 2827-2839, 1994.
29
30

31
32
33
34 **Jacobs KM, Kharazia VN, and Prince DA.** Mechanisms underlying epileptogenesis in
35 cortical malformations. *Epilepsy Res* 36:165-88, 1999.
36
37

38
39
40
41 **Köhling R.** Voltage-gated sodium channels in epilepsy. *Epilepsia* 43: 1278-1295, 2002.
42
43

44
45
46 **Krimer LS and Goldman-Rakic PS.** Prefrontal microcircuits: Membrane properties and
47 excitatory input of local, medium and wide arbor interneurons *J Neurosci* 21: 3788–3796,
48
49
50
51 2001.
52
53
54
55
56
57
58
59
60

BURSTING ACTIVITY IN NEOCORTICAL NETWORKS

1
2
3 **Marder E, Calabrese RL.** Principles of rhythmic motor pattern generation. *Physiol Rev.*
4
5 76:687-717, 1996.
6
7

8
9
10 **Mountcastle VB.** The columnar organization of the neocortex,” *Brain* 120: 701–722,
11
12 1997.
13

14
15
16
17 **Nieuwenhuys R.** The neocortex: An overview of its evolutionary development, structural
18 organization and synaptology. *Anat Embryol* 190: 307–337, 1994.
19
20

21
22
23
24 **Nowak LG, Azouz R, Sanchez-Vives MV, Gray CM, and McCormick DA.**
25
26
27 Electrophysiological classes of cat primary visual cortical neurons in vivo as revealed by
28
29 quantitative analyses. *J Neurophysiol* 89:1541-66, 2003.
30
31

32
33
34 **Nunez PL.** *Electric Fields of the Brain: The Neurophysics of EEG.* Oxford: Oxford
35
36 University Press, 1981.
37
38

39
40
41 **Peña F and Ramirez JM.** Endogenous activation of serotonin-2A receptors is required
42
43 for respiratory rhythm generation in vitro. *J Neurosci* 22:11055-11064, 2002.
44
45

46
47
48 **Peña F and Ramirez JM.** Substance P-mediated modulation of pacemaker properties in
49
50 the mammalian respiratory network. *J Neurosci* 24:7549-7556, 2004.
51
52

BURSTING ACTIVITY IN NEOCORTICAL NETWORKS

1
2
3 **Ramirez JM, Tryba AK, and Peña F.** Pacemaker neurons and neuronal networks: an
4 integrative view. *Curr Opin Neurobiol* 14:665-674, 2004.
5
6
7

8
9
10 **Sanabria ER, da Silva AV, Spreafico R, and Cavalheiro EA.** Damage, reorganization,
11 and abnormal neocortical hyperexcitability in the pilocarpine model of temporal lobe
12 epilepsy. *Epilepsia*;43 Suppl 5:96-106, 2002.
13
14
15

16
17
18 **Sanabria ER, Su H, and Yaari Y.** Initiation of network bursts by Ca²⁺-dependent
19 intrinsic bursting in the rat pilocarpine model of temporal lobe epilepsy. *J Physiol.* 532:
20 205-216, 2001.
21
22
23

24
25
26 **Sanchez-Vives MV and McCormick DA.** Cellular and network mechanisms of
27 rhythmic recurrent activity in neocortex. *Nat Neurosci* ;3:1027-1034, 2000.
28
29
30

31
32
33 **Schwindt P and Crill W.** Mechanisms underlying burst and regular spiking evoked by
34 dendritic depolarization in layer 5 cortical pyramidal neurons. *J Neurophysiol* 81:1341-
35 1354, 1999.
36
37
38

39
40
41 **Somogyi P, Tamas G, Lujan R, and Buhl EH.** Salient features of synaptic organization
42 in the cerebral cortex. *Brain Res Rev* 26:113-35, 1998.
43
44
45

BURSTING ACTIVITY IN NEOCORTICAL NETWORKS

1
2
3 **Staley KJ, Bains JS, Yee A, Hellier J, and Longacher JM.** Statistical model relating
4 CA3 burst probability to recovery from burst-induced depression at recurrent collateral
5 synapses. *J Neurophysiol* 86:2736-2747, 2001.
6
7
8
9

10
11
12 **Staiger JF, Schubert D, Zuschratter W, Kotter R, Luhmann HJ, and Zilles K.**
13 Innervation of interneurons immunoreactive for VIP by intrinsically bursting pyramidal
14 cells and fast-spiking interneurons in infragranular layers of juvenile rat neocortex. *Eur J*
15 *Neurosci* 16:11-20, 2002.
16
17
18
19
20
21

22
23
24 **Steriade M.** Neocortical cell classes are flexible entities. *Nat Rev Neurosci* 5:121-34,
25 2004.
26
27
28
29

30
31 **Steriade M and Amzica F.** Sleep oscillations developing into seizures in corticothalamic
32 systems. *Epilepsia* 44 Suppl 12:9-20, 2003.
33
34
35
36

37
38 **Steriade M, Timofeev I, Grenier F, and Durmuller N.** Role of thalamic and cortical
39 neurons in augmenting responses and self-sustained activity: dual intracellular recordings
40 in vivo. *J Neurosci* 18:6425-43, 1998.
41
42
43
44
45

46
47
48 **Steriade M, Timofeev I, and Grenier F.** Natural waking and sleep states: a view from
49 inside neocortical neurons. *J Neurophysiol* 85:1969-1985, 2001.
50
51
52
53
54
55

BURSTING ACTIVITY IN NEOCORTICAL NETWORKS

1
2
3 **Steriade M, Amzica F, Neckelmann D, and Timofeev I.** Spike-wave complexes and
4 fast components of cortically generated seizures. II. Extra- and intracellular patterns.
5
6

7
8 *J Neurophysiol* 80:1456-79, 1998.
9

10
11
12 **Timofeev I, Grenier F, and Steriade M.** Impact of intrinsic properties and synaptic
13 factors on the activity of neocortical networks in vivo. *J Physiol Paris* 94:343-355, 2000.
14
15
16

17
18
19 **Timofeev I and Steriade M.** Neocortical seizures: initiation, development and cessation.
20
21
22 *Neuroscience* 123:299-336, 2004.
23

24
25
26
27 **Topolnik L, Steriade M, and Timofeev I.** Hyperexcitability of intact neurons underlies
28 acute development of trauma-related electrographic seizures in cats in vivo. *Eur J*
29
30
31 *Neurosci* 18:486-96, 2003.
32

33
34
35
36 **Traub RD, Whittington MA, Buhl EH, LeBeau FE, Bibbig A, Boyd S, Cross H, and**
37
38 **Baldeweg T.** A possible role for gap junctions in generation of very fast EEG oscillations
39 preceding the onset of, or perhaps initiating, seizures. *Epilepsia* 42 : 153–170, 2001.
40
41
42

43
44
45
46 **Traub RD, Buhl EH, Gloveli T, and Whittington MA.** Fast rhythmic bursting can be
47 induced in later 2/3 cortical neurons by enhancing persistent Na⁺ conductance or by
48
49 blocking BK channels. *J Neurophysiol* 89: 909–921, 2003.
50
51
52

BURSTING ACTIVITY IN NEOCORTICAL NETWORKS

1
2
3 **Traub RD, Contreras D, Cunningham MO, Murray H, LeBeau FE, Roopun A,**
4 **Bibbig A, Wilent WB, Higley MJ, and Whittington MA.** Single-column
5
6 thalamocortical network model exhibiting gamma oscillations, sleep spindles, and
7
8 epileptogenic bursts. *J Neurophysiol* 93:2194-2232, 2005.
9
10

11
12
13
14
15 **Traub RD, Jefferys JGR, Miles R, Whittington MA, and Toth, K.** A branching
16
17 dendritic model of a rodent CA3 pyramidal neurone. *J. Physiol* 481: 79-95, 1994.
18
19

20
21
22 **Van Drongelen W, Koch H, Marcuccilli C, Peña F and Ramirez JM.** Synchrony
23
24 levels during evoked seizure-like bursts in mouse neocortical slices. *J Neurophysiol* 90:
25
26 1571-1580, 2003a.
27
28

29
30
31 **Van Drongelen W, Koch H, Peña F, Tryba A, Parkis M, Loweth J, Hecox KE,**
32 **Kohrman M, Frim D, Chico MS, Ramirez JM, and Marcuccilli CJ.** Differences in
33
34 bursting properties between least and most abnormal tissue obtained from pediatric
35
36 patients with intractable epilepsy. *Abstract Viewer/Itinerary Planner Washington DC:*
37
38 *Society for Neuroscience*, No. 99.15.2003 , 2003b.
39
40
41
42
43

44
45
46 **Van Drongelen W, Lee HC, Hereld M, Jones D, Cohoon M, Elsen F, Papka ME, and**
47 **Stevens RL.** Simulation of neocortical epileptiform activity using parallel computing.
48
49 *Neurocomputing* 58-60: 1203-1209, 2004.
50
51
52
53
54
55
56
57
58
59
60

BURSTING ACTIVITY IN NEOCORTICAL NETWORKS

1
2
3 **Van Drongelen W, Lee HC, Koch, Hereld M, Elsen F, Chen Z, and Stevens RL.**

4
5
6 Emergent epileptiform activity in neural networks with weak excitatory synapses. *IEEE*

7
8 *Trans Neur Sy. & Rehab* 13: 236-241, 2005.
9
10
11
12
13
14
15
16
17
18
19
20
21
22
23
24
25
26
27
28
29
30
31
32
33
34
35
36
37
38
39
40
41
42
43
44
45
46
47
48
49
50
51
52
53
54
55
56
57
58
59
60

For Peer Review

BURSTING ACTIVITY IN NEOCORTICAL NETWORKS

APPENDIX

The overall approach to our modeling effort in this study was first to determine acceptable cellular behavior first and then to obtain emergent network behavior. To determine the part of parameter space that would create the desired cellular behavior, we first determined the voltage sensitivity of the sodium and potassium channels by using the literature values originally reported by Hodgkin and Huxley (1952), and our recorded set for N_{ap} (Fig. 3). The compartment sizes (Table 1) were based on cellular dimensions and a procedure to collapse cellular parts into single cylindrical compartments (Bush and Sjenowski 1993; Van Drongelen et al. 2004, 2005). Because the model's surface areas represent an estimate, the maximum levels of conductivity were determined in a brute force parameter search of 58,644 simulations. For regular and fast spiking cells, the target was to obtain spiking at different levels of current injection (Fig. 8) and no spontaneous activity at a normal resting potential. The cells, including N_{ap} current, were adjusted to show bursting behavior during rest and moderate current injection levels. At higher levels of current injection the behavior transitioned into beating behavior (Butera et al. 1999). We evaluated the following parameter ranges; the values we selected for the simulations reported here are indicated in parentheses:

1. Membrane resistance: 0.1–5.0 Ωm^2 (5 and 0.1 for the axon/initial segment)
2. Axial intracellular resistance: 0.3–10 Ωm (2 and 1 for the axon/initial segment)
3. Maximum fast sodium conductance in the soma: 300–3000 S/m² (2000)
4. Maximum persistent sodium conductance in the soma: 0.3–350 S/m² (65)
5. Maximum potassium conductance in the soma: 6–1000 S/m² (650)

BURSTING ACTIVITY IN NEOCORTICAL NETWORKS

- 1
2
3
4
5
6
7
8
9
10
11
12
13
14
15
16
17
18
19
20
21
22
23
24
25
26
27
28
29
30
31
32
33
34
35
36
37
38
39
40
41
42
43
44
45
46
47
48
49
50
51
52
53
54
55
56
57
58
59
60
6. Maximum fast sodium conductance in the initial segment/axon: 30–100,000 S/m²
(6000)
7. Maximum potassium conductance in the initial segment/axon: 6–100,000 S/m²
(2000)

Membrane capacitance was 0.01 F/m². Gap junctions had a resistance of 200 MΩ, a value representing 5 gap junctions with a 1 nS conductivity for each (Traub et al. 2005). In spite of common belief that one may easily simulate any type of activity pattern with the rich parameter set of biophysically realistic models, the large number of parameters is more an obstruction than a facilitator for finding the part of parameter space associated with acceptable behavior; in our example above we found about 0.05% of the simulations generated the desired, realistic behavior. This set was not distributed over the parameter space but encompassed a small area showing desired spontaneous bursting; this area was located around the parameter choice indicated in parentheses in the list above.

As the next step in defining the network, we connected the cells according to the diagrams in Fig. 1. By evaluating a wide range of synaptic strength parameters for the individual synapse model in a brute force parameter search, we adjusted the synaptic strength to obtain desynchronized network bursting behavior (Van Drongelen et al. 2005). The synaptic connectivity parameters based on values reported for mammalian cortex are summarized in Table 2.

BURSTING ACTIVITY IN NEOCORTICAL NETWORKS

LEGENDS

Fig. 1

Diagram of the computational model of neocortex. Superficial pyramidal cells (S) and deep pyramidal cells (D) are located in different layers. The interneurons (I) are inhibitory cells located in a third layer.

(A) Excitatory connections between pyramidal cells and between pyramidal cells and interneurons. Interneurons of each type are interconnected with gap junctions (R).

Parameters associated with the excitatory connections indicated by 1-14 can be found in Table 2 in the Appendix.

(B) Inhibitory connectivity between basket cells (B) and the soma of the pyramidal neurons and between chandelier cells (C) and the initial segment of the pyramidal neurons. Inhibitory connections indicated by a-h and disinhibition I-IX correspond to Table 2 in the Appendix.

Fig. 2.

Recording techniques. (A) Extracellular and intracellular electrodes are placed in close proximity in the neocortical slice. (B) Population activity is recorded extracellularly, and a rectifier plus integrator is used to emphasize burst activity of the network. (C) Current clamp measurement shows the activity pattern of individual pyramidal neurons associated with the population bursts. (D) Voltage clamp measurement was applied to evaluate sodium currents in the cell membrane and to measure postsynaptic current.

BURSTING ACTIVITY IN NEOCORTICAL NETWORKS

Fig. 3.

1
2
3
4
5
6
7
8
9
10
11
12
13
14
15
16
17
18
19
20
21
22
23
24
25
26
27
28
29
30
31
32
33
34
35
36
37
38
39
40
41
42
43
44
45
46
47
48
49
50
51
52
53
54
55
56
57
58
59
60

A) Voltage-activated sodium current response traces to different test potentials (Inset: Holding potential: -80 mV, 10 mV steps from -90 to 20 mV, step duration: 150 ms). We measured the persistent sodium (I_{NaP}) current amplitudes at the steady state level as indicated by the filled circle. The figure shows cortical pyramidal neuron with attached patch pipette. B) Current/voltage relationship diagram (I/V-curve) of persistent sodium current (I_{NaP}) (n=43) and I_{NaP} after bath application of 20 μ M riluzole. The average current amplitude values are plotted against the respective test potentials. C) Normalized current amplitudes of I_{NaP} , I_{NaP} + riluzole (20 μ M, n=5) and I_{NaP} + TTX (50 nM, n=7). All absolute values were normalized to the respective maximal I_{NaP} current amplitude (I/I_{max}). D) Inactivation test protocol: Example of I_{NaP} current response traces to a test potential of -15 mV (peak voltage range) after different holding potentials (10 seconds) from -20 to -120 mV (10 mV steps). The still activatable I_{NaP} current amplitudes were measured at the steady-state level as indicated by the open circle. E) Average activation and inactivation curves for I_{NaP} . Activation parameters (filled circles) are plotted as normalized conductance values (right y-axis) against the respective test potentials (V_t). Inactivation parameters (open circles) are plotted as normalized current amplitudes from 28 I_{NaP} inactivation measurements (left y-axis) against the respective V_t . Sigmoidal Boltzman fits through both sets of data points deliver the activation parameters $V_{50} = -46.2 \pm 1.4$ mV and slope = 9.9 ± 1.3) and inactivation parameters $V_{50} = -64.4 \pm 2.3$ mV and slope = 19.0 ± 2.5 for I_{NaP} . F) Activation parameter comparison between I_{NaP} , I_{NaP} + riluzole (20 μ M), and I_{NaP} + TTX (50nM). Sigmoidal Boltzman fits through the data sets

BURSTING ACTIVITY IN NEOCORTICAL NETWORKS

1
2
3 deliver the following activation parameters: $\text{Na}_p + \text{riluzole}$: $V_{50} = -49.6 \pm 2.8$ mV and
4
5 slope = 4.8 ± 2.8 ; and $\text{Na}_p + \text{TTX}$: $V_{50} = -48.6 \pm 3.0$ mV and slope = 5.6 ± 4.1 .
6
7
8
9

Fig. 4

10
11
12 Synaptic activity before and after adding riluzole (20 μM). First the action potential
13
14 generation mechanism was disabled with TTX (1 μM), and the control synaptic activity
15
16 was measured; then the effect of riluzole was determined. (B) Example miniature
17
18 excitatory postsynaptic current traces (mEPSCs) during control conditions (TTX) and
19
20 after additional application of riluzole (RIL). The traces presented here are examples of
21
22 average current traces from 50 single events of a 4-minute recording during the
23
24 respective conditions. (C) Comparison of the decay time constants (τ) and amplitudes of
25
26 mEPSCs during control (TTX) and riluzole (RIL) conditions. Time constants and
27
28 amplitudes were determined by a single exponential fit through the decay phase of the
29
30 average mEPSCs (see the Methods section). The changes for τ and amplitude were not
31
32 significantly different.
33
34
35
36
37
38
39
40
41

Fig. 5

42
43
44 Neuronal activity of the population (upper traces in each panel) usually showed a
45
46 relationship with the individual neuron (lower traces). In regular spiking (RS) neurons (A
47
48 panels) and bursting (IB) neurons (B panels), we found three types of activity associated
49
50 with the population burst: excitation (A1, B1), a combination of excitation followed by a
51
52 phase of inhibition (A2, B2), or inhibition (A3, B3). A subclass of bursting cells
53
54
55
56
57
58
59
60

BURSTING ACTIVITY IN NEOCORTICAL NETWORKS

1
2
3 remained active after the network effect was removed by bath application of CPP and
4
5
6 CNQX.
7
8
9

Fig. 6

10
11
12 Responses of a representative RS (A1) and IB (A2, A3) neurons to current injection (100
13
14 pA, lower traces) before and after riluzole (A1, A2) or a low-concentration TTX (A3)
15
16 was added to the ACSF. Application of riluzole or TTX inhibited the intrinsic bursting
17
18 properties of the IB type cells; firing of the RS was not significantly altered. (B) The
19
20 instantaneous spike frequency plotted against time elapsed since stimulus onset for the
21
22 neurons is shown in (A). The lines represent the frequency before adding riluzole, the
23
24 dotted lines after adding riluzole measured immediately after the network stopped
25
26 bursting. At the cessation of network bursting, the IB neurons exhibited regular spiking
27
28 activity like the RS type cell. Losing the bursting property was associated with a
29
30 reduction of action potentials per second. Histograms in (C) show the overall the change
31
32 in response expressed in the number of action potentials in the first second after onset of
33
34 current injection of (C1) RS (n=8) and (C2) IB neurons (n=4) before adding riluzole
35
36 (CTRL) and the effect of riluzole after the network stopped bursting (RIL). The effects
37
38 for low concentrations of TTX on RS (n=4) and IB (n=4) type cells were identical. For
39
40 the RS neurons, no significant difference was observed; the difference for the IB type
41
42 neuron was significant ($p < .05$).
43
44
45
46
47
48
49
50
51
52
53
54
55
56
57
58
59
60

BURSTING ACTIVITY IN NEOCORTICAL NETWORKS

Fig. 7

A) Effect of riluzole (20 μ M) on network bursting frequency. Extracellular network activity was recorded for up to 10 minutes after drug application, and the number of bursts was recorded in 50 second intervals. **B)** Effect of riluzole (20 μ M) on the action potential firing rate of regular spiking (n=8, open triangle) and intrinsic bursting neurons (n=4, open square). Rates were determined for 30-second intervals. **C)** Effect of riluzole (20 μ M) on the amplitude of persistent sodium current (I_{NaP}). The maximal I_{NaP} amplitude was determined every ten seconds by a single voltage step from -80 to -20 mV. One hundred percent was determined by the average from the last three measurements before onset of riluzole application. **D)** Effect of low tetrodotoxin concentration (TTX, 50 nM) on network bursting frequency. Extracellular network activity was recorded for up to 10 minutes after drug application and the number of bursts was recorded in 50 second intervals. **E)** Effect of low-tetrodotoxin concentration (TTX, 50 nM) on the action potential firing rate of regular spiking (n=4, open triangle) and intrinsic bursting neurons (n=4, open square). Rates were determined for 30-second intervals. **F)** Effect of low tetrodotoxin concentration (TTX, 50 nM) on the amplitude of persistent sodium current. The maximal I_{NaP} amplitude was determined every 10 seconds by a single voltage step from -80 to -20 mV. One hundred percent was determined by the average from the last three measurements before onset of TTX application.

Note: Since cellular + network activity was recorded with a different system from the voltage clamp data; there is a 60-second difference in latency between drug administration and arrival in the bath. For this reason there is a 60-second shift of the graphs in C) and F) relative to the other ones!

BURSTING ACTIVITY IN NEOCORTICAL NETWORKS

Fig. 8

Simulation results obtained for single cell and network activity; the patterns evoked by current injections in RS and IB types of the cell models included in the network simulation. The upper trace in each panel shows the action potential activity; the lower trace indicates onset and level of current injected in the cell soma. In order to show similar responses, the level of current injection was adapted for each cell type. Panels A-D show responses of superficial and deep pyramidal neurons; E-H show activity from three types of basket cell and the axo-axonic interneuron (chandelier cell). Except for the bursting cells (A and C) that included a persistent sodium current, all neuron types had regular spiking characteristics. Compared to the pyramidal neurons, the smaller basket cells (E-G) and the chandelier cell (H) spiked at a lower threshold of current. Within the pyramidal neuron population, the larger deep cells (D) showed a higher threshold compared to that of the superficial neurons (B). (I) Network activity in the computational network. The raw network activity (top trace) and integrated activity (bottom trace) are the simulated equivalents of the traces in Fig. 2B. The computational results show that bursting activity of the network stops after reducing the Na_p conductivity in the time interval indicated by the horizontal bar. (J) Recorded integrated network activity in a slice where riluzole was added to the ACSF.

Table 1

Overview of cell compartments, compartment size, associated voltage sensitive ion channels, synaptic channels and gap junctions .

BURSTING ACTIVITY IN NEOCORTICAL NETWORKS

Table 2

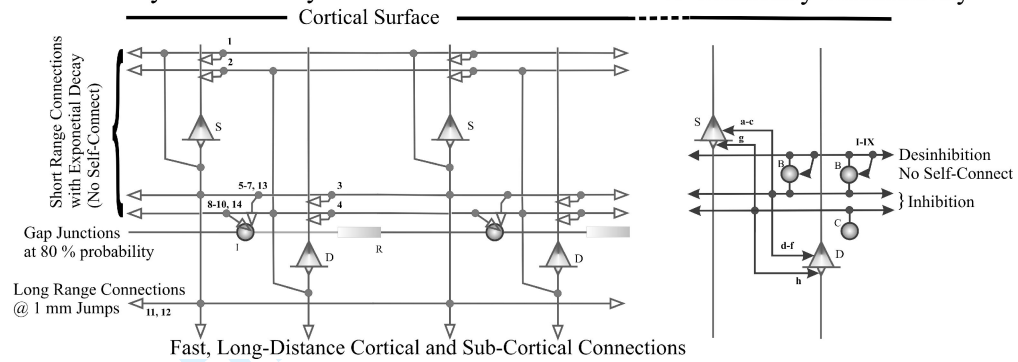
Overview of the connectivity parameters in the simulation. The identifications in the left column correspond with the connections in the diagrams in Fig. 1.

Delete before publication.

The submitted manuscript has been created by the University of Chicago as Operator of Argonne National Laboratory (“Argonne”) under Contract No. W-31-109-ENG-38 with the U.S. Department of Energy. The U.S. Government retains for itself, and others acting on its behalf, a paid-up, nonexclusive, irrevocable worldwide license in said article to reproduce, prepare derivative works, distribute copies to the public, and perform publicly and display publicly, by or on behalf of the Government. This government license should not be published with the paper.

A Excitatory Connectivity

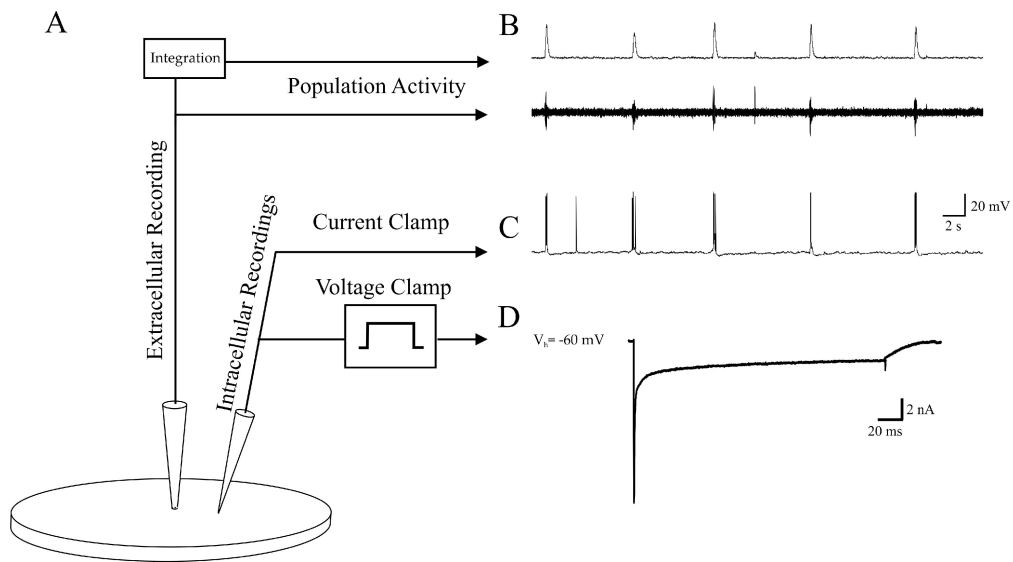
B Inhibitory Connectivity



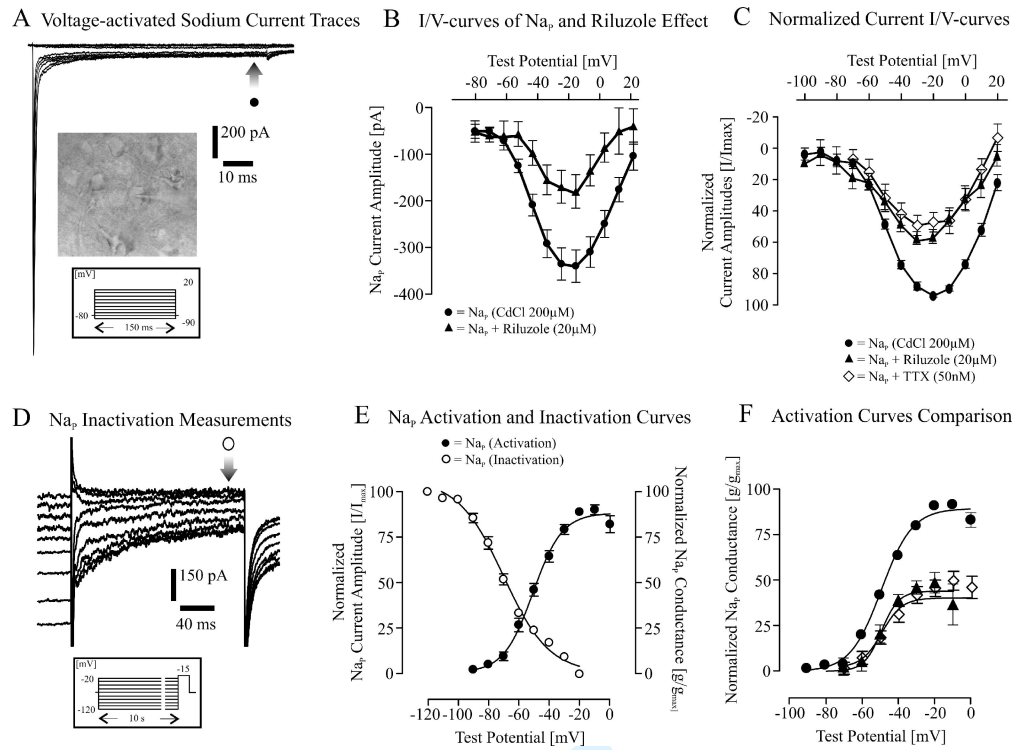
Preprint Peer Review

1
2
3
4
5
6
7
8
9
10
11
12
13
14
15
16
17
18
19
20
21
22
23
24
25
26
27
28
29
30
31
32
33
34
35
36
37
38
39
40
41
42
43
44
45
46
47
48
49
50
51
52
53
54
55
56
57
58
59
60

1
2
3
4
5
6
7
8
9
10
11
12
13
14
15
16
17
18
19
20
21
22
23
24
25
26
27
28
29
30
31
32
33
34
35
36
37
38
39
40
41
42
43
44
45
46
47
48
49
50
51
52
53
54
55
56
57
58
59
60

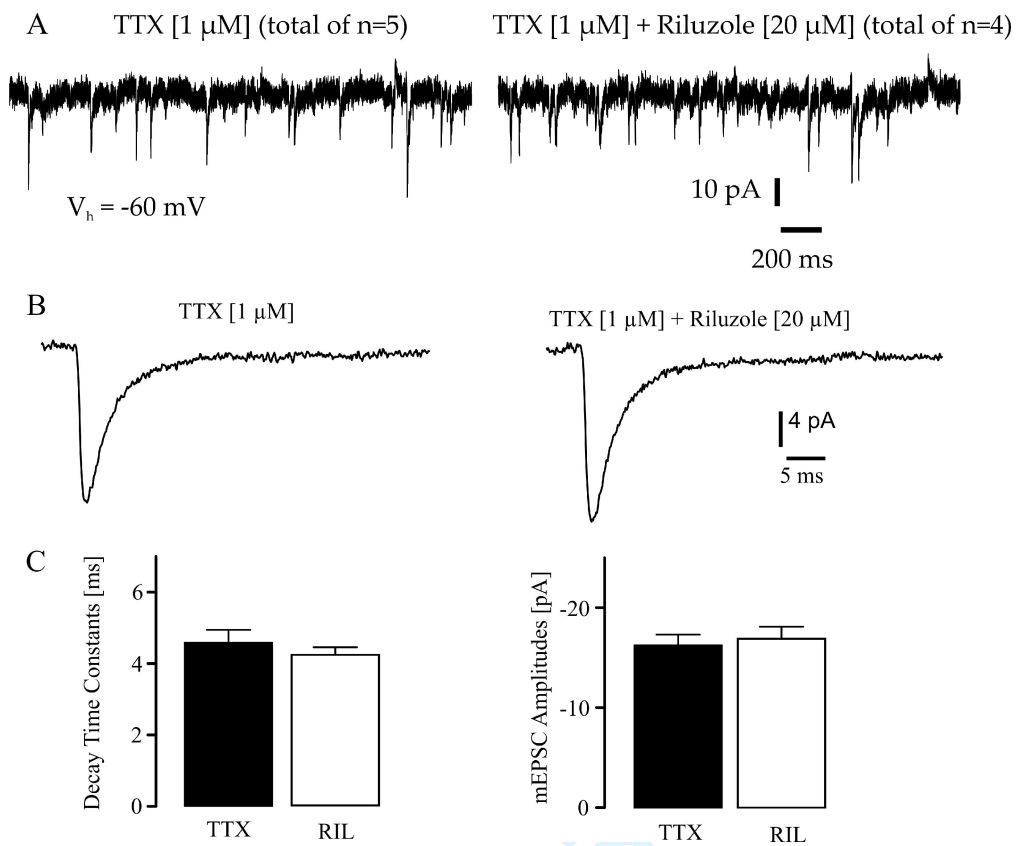


Peer Review

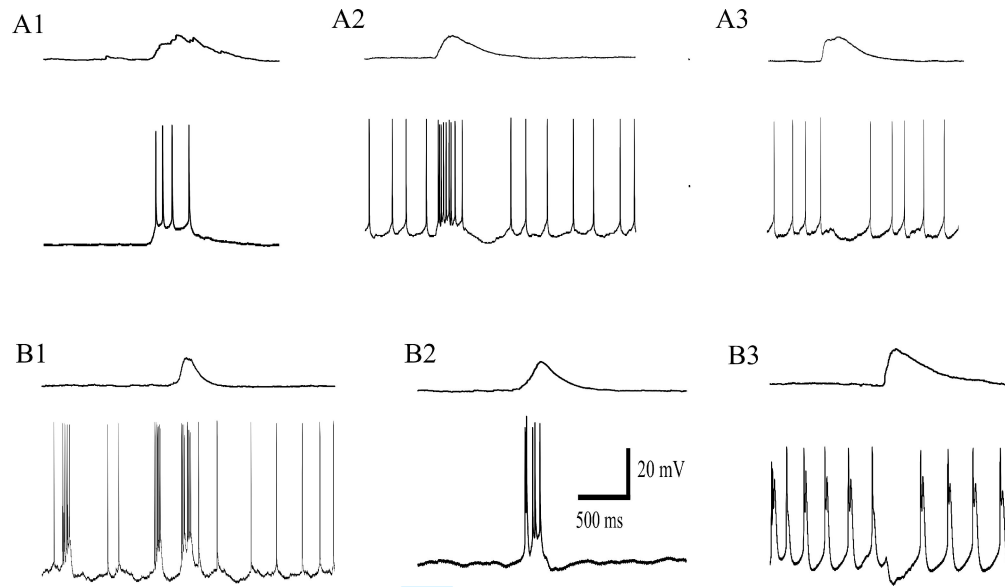


Review

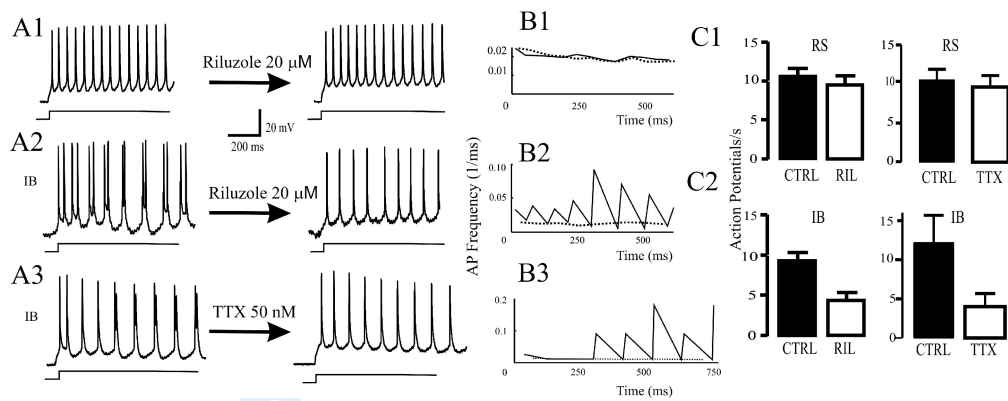
1
2
3
4
5
6
7
8
9
10
11
12
13
14
15
16
17
18
19
20
21
22
23
24
25
26
27
28
29
30
31
32
33
34
35
36
37
38
39
40
41
42
43
44
45
46
47
48
49
50
51
52
53
54
55
56
57
58
59
60



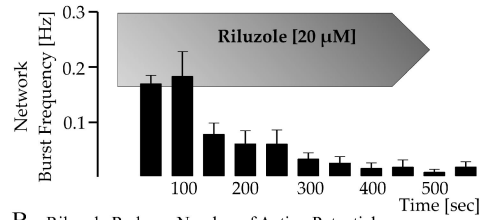
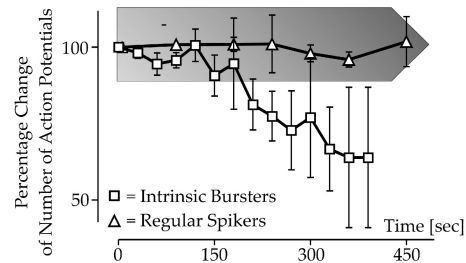
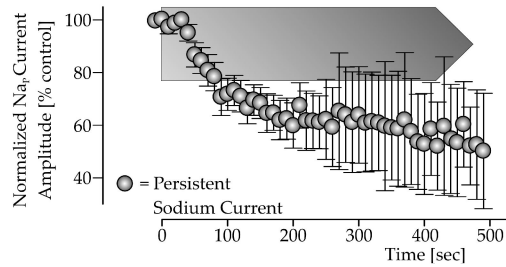
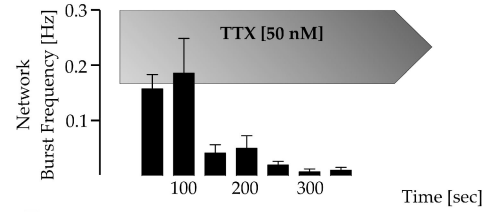
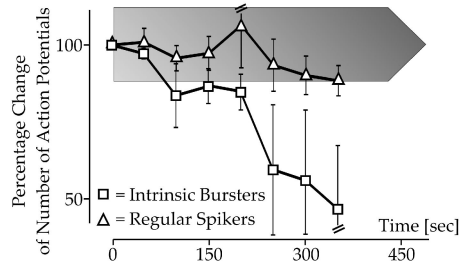
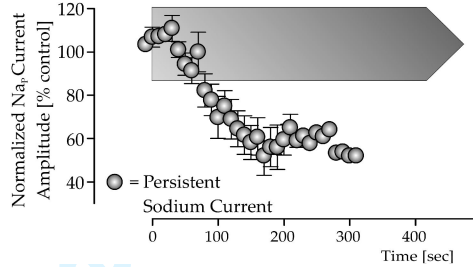
review



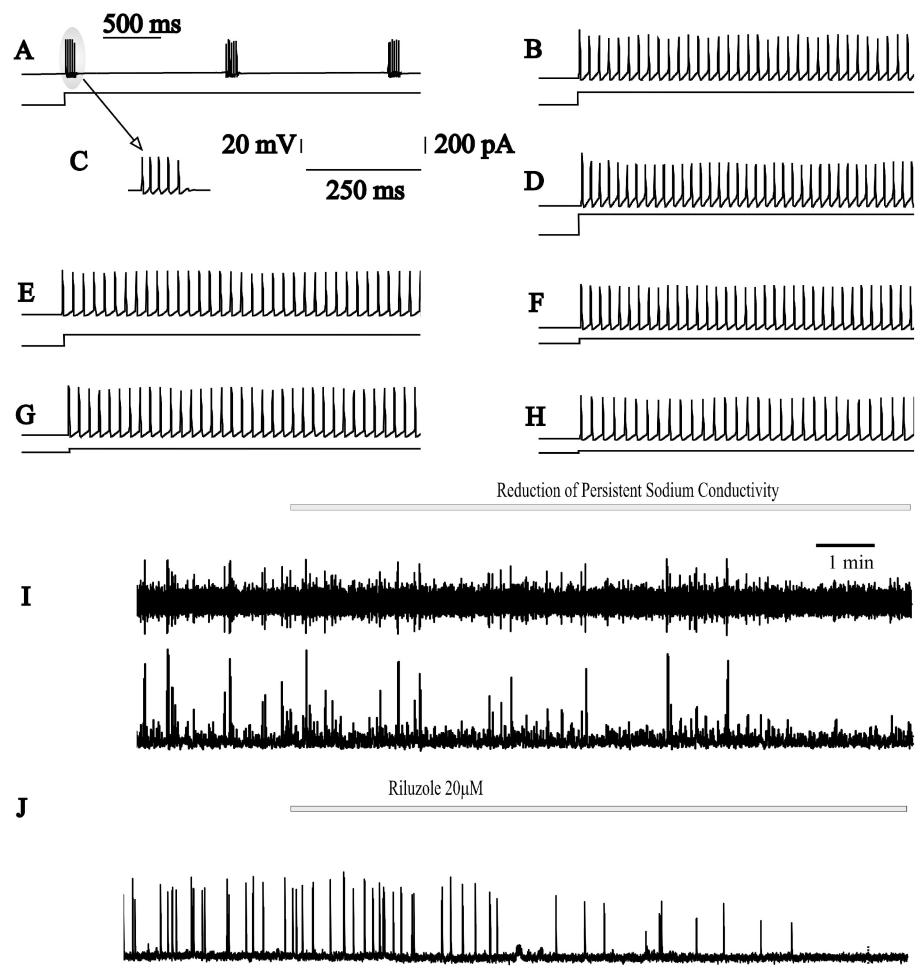
1
2
3
4
5
6
7
8
9
10
11
12
13
14
15
16
17
18
19
20
21
22
23
24
25
26
27
28
29
30
31
32
33
34
35
36
37
38
39
40
41
42
43
44
45
46
47
48
49
50
51
52
53
54
55
56
57
58
59
60



Or Peer Review

A Riluzole Reduces Network Burst Frequency**B** Riluzole Reduces Number of Action Potentials in Intrinsic Bursters**C** Riluzole Reduces Na_v Current Amplitude**D** Low TTX Reduces Network Burst Frequency**E** Low TTX Reduces Number of Action Potentials in Intrinsic Bursters**F** Low TTX Reduces Na_v Current Amplitude

1
2
3
4
5
6
7
8
9
10
11
12
13
14
15
16
17
18
19
20
21
22
23
24
25
26
27
28
29
30
31
32
33
34
35
36
37
38
39
40
41
42
43
44
45
46
47
48
49
50
51
52
53
54
55
56
57
58
59
60



EW

Table 1

Overview of cell compartments, compartment size, associated voltage sensitive ion channels, synaptic channels and gap junctions .

Cell - Compartment	Size (μm)	V-Channels	Synapse
S_PYRAMIDAL-soma	22, 16.1	Na, K, NaP	i
- sd1	140, 2	-	-
- sd2	190, 3.3	-	e
- bd	200, 2.4	-	-
- is	50, 2.2	Na, K	i
D_PYRAMIDAL-soma	22, 16.1	Na, K	i
- dd1	250, 2	-	-
- dd2	400, 2.9	-	-
- dd3	400, 4.4	-	e
- dd4	400, 4.7	-	-
- bd	200, 6.3	-	-
- is	50, 2.2	Na, K	i
BASKET1-3-soma	5.5-22, 4-16.1	Na, K	e, i
- d	300-900, 2	-	gj
CHANDELIER-soma	5.5, 4	Na, K	e, i
- d	150, 2	-	gj

Table 2

Overview of the connectivity parameters in the simulation. The identifications in the left column correspond with the connections in the diagrams in Fig. 1.

# and Ref	Synapse	Destination (um)	Source hole (um)	Probability	Exponential in x, y only (um)	Velocity +/- (m/s)	Max W	Min W	Exponential in 3D (um)
1	Exc: S_PYR → S_PYR	500	5, 5, 1500(*)	0.10	300	0.08 (25%)	6	0	200
2	Exc: D_PYR → S_PYR	500	-	0.10	300	0.08 (25%)	6	0	1500
3	Exc: S_PYR → D_PYR	500	-	0.10	300	0.08 (25%)	6	0	1500
4	Exc: D_PYR → D_PYR	500	5, 5, 1500	0.10	300	0.08 (25%)	6	0	200
5	Exc: S_PYR → BASK1	100	-	0.25	10,000	0.08 (25%)	1	1	10,000
6	Exc: S_PYR → BASK2	100	-	0.25	10,000	0.08 (25%)	1	1	10,000
7	Exc: S_PYR → BASK3	100	-	0.25	10,000	0.08 (25%)	1	1	10,000
8	Exc: D_PYR → BASK1	100	-	0.25	10,000	0.08 (25%)	1	1	10,000
9	Exc: D_PYR → BASK2	100	-	0.25	10,000	0.08 (25%)	1	1	10,000
10	Exc: D_PYR → BASK3	100	-	0.25	10,000	0.08 (25%)	1	1	10,000
11	Exc: S_PYR → S_PYR < 1cm, every 1mm, 200um	5, 5, 1500	5, 5, 1500	0.10	-	15 (95%)	3	3	1000,000
12	Exc: S_PYR → D_PYR < 1cm, every 1mm, 200um	5, 5, 1500	5, 5, 1500	0.10	-	15 (95%)	3	3	1000,000
13	Exc: S_PYR → CHAND	100	-	0.25	10,000	0.08 (25%)	.5	.5	10,000
14	Exc: D_PYR → CHAND	100	-	0.25	10,000	0.08 (25%)	.5	.5	10,000
a	Inh: BASK1 → S_PYR	300	-	0.04	300	0.08 (25%)	6	6	10,000
b	Inh: BASK2 → S_PYR	600	-	0.01	600	0.08 (25%)	6	6	10,000
c	Inh: BASK3 → S_PYR	900	-	0.005	900	0.08 (25%)	6	6	10,000
d	Inh: BASK1 → D_PYR	300	-	0.04	300	0.08 (25%)	6	6	10,000
e	Inh: BASK2 → D_PYR	600	-	0.01	600	0.08 (25%)	6	6	10,000
f	Inh: BASK3 → D_PYR	900	-	0.005	900	0.08 (25%)	6	6	10,000
g	Inh: CHAND → S_PYR	300	-	0.04	300	0.08 (25%)	1	0	10,000
h	Inh: CHAND → D_PYR	300	-	0.04	300	0.08 (25%)	1	0	10,000
I	Dinh: BASK1 → BASK1	300	5, 5, 1500	0.04	300	0.08 (25%)	1	1	10,000
II	Dinh: BASK1 → BASK2	300	5, 5, 1500	0.04	300	0.08 (25%)	1	1	10,000
III	Dinh: BASK1 → BASK3	300	5, 5, 1500	0.04	300	0.08 (25%)	1	1	10,000
IV	Dinh: BASK2 → BASK1	600	5, 5, 1500	0.015	600	0.08 (25%)	1	1	10,000
V	Dinh: BASK2 → BASK2	600	5, 5, 1500	0.015	600	0.08 (25%)	1	1	10,000
VI	Dinh: BASK2 → BASK3	600	5, 5, 1500	0.015	600	0.08 (25%)	1	1	10,000
VII	Dinh: BASK3 → BASK1	900	5, 5, 1500	0.007	900	0.08 (25%)	1	1	10,000
VIII	Dinh: BASK3 → BASK2	900	5, 5, 1500	0.007	900	0.08 (25%)	1	1	10,000
IX	Dinh: BASK3 → BASK3	900	5, 5, 1500	0.007	900	0.08 (25%)	1	1	10,000